Semiconductor Bloch Equations

Ralph v. Baltz
Institut für Theorie der Kondensierten Materie
Karlsruher Institut für Technologie (KIT), Germany

1 Introduction

The electrodynamic description of matter requires constitutive equations which relate the induced charge ρ and current density $\mathbf{j}$ of the semiconductor (or, equivalently, the polarization $\mathbf{P}$, with $\mathbf{j} = \dot{\mathbf{P}}$ and $\rho = -div\ \mathbf{P}$) to the electromagnetic fields $\mathbf{E}, \mathbf{B}$. Generic models in this respect are the Lorentz–oscillator and the Drude–free–carrier model of linear optics. The description of nonlinear properties of matter, on the other hand, mostly uses a power series expansion of the polarization in terms of the electrical field, such an expansion, however, is inappropriate under resonant or near resonant conditions. In some cases new solutions may even arise "spontaneously" above a critical light field and can lead to second harmonic generation although a power expansion (including even–order terms with respect to the light field) does not exist. Therefore, a realistic description of semiconductor optics requires the proper dependence on the light field, the inclusion of the valence–conduction band continuum states, exciton effects, as well as band–filling dynamics. These phenomena are consistently described by the *Semiconductor Bloch–Equations* (SBE's) which nowadays became the *standard model* of semiconductor optics.[1] In this approach the semiconductor is treated quantum mechanically which leads to a set of coupled nonlinear differential equations for the polarization and the electron/hole distribution functions (supplemented by higher order correlation functions which will be omitted here). The polarization acts then as a source term in the (classical) Maxwell–equations. In this sense the SBE's are a semiclassical theory. It successfully covers linear as well as nonlinear phenomena such as pump–probe, four–wave–mixing, or photon–echo experiments, as discussed in Ref.[24K1] (Vol. 2).

The SBE's are of considerable complexity in derivation and application, therefore, we shall give only a "pedestrian version" of their derivation and some selected applications. Details can be found in Haug and Koch's texbook[94H1]. For a comprehensive presentation of the SBE's see, e.g., Schäfer and Wegener's book[02S1]. We approach the problem in three steps as sketched in Fig. 1.

(a) First we study the dynamics of atoms near resonance in the two–level approximation and derive the optical Bloch equations. In this formulation, damping

[1] This article is a shortened version of Sects. 4 and 11.4.1 of Ref. [24K1] (Vol. 2). The main idea of the SBE's originates from Bloch's seminal work on the theory of (nuclear) spin resonance[46B1] and Haken's theory of the Laser[70H1]. For semiconductors, "band edge equation" were first studied by Stahl[84S1] and, subsequently, developed by Haug and his school[94H1] and others to a powerful tool of semiconductor theory.

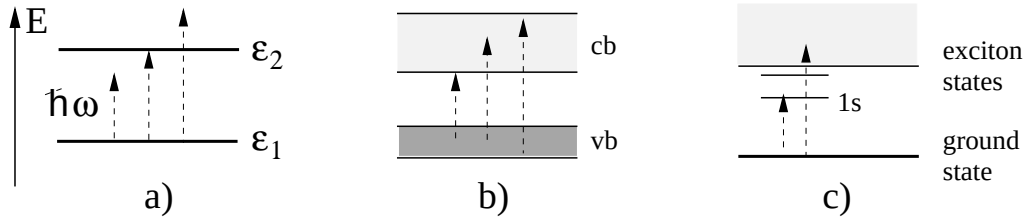

Figure 1: Route for a qualitative "derivation" of the the Semiconductor Bloch equations. (a) Two–Level system (resonant and nonresonant excitation), (b) noninteracting valence and conduction bands viewed as a collection of TLS's with different transition energies, and (c) two interacting bands including some bound exciton states.

processes can also be included on a phenomenological level.

(b) Second, we generalize this result for a two–band model of a direct semiconductor omitting the Coulomb interaction between electrons and holes. In this description the semiconductor is sketched as a collection of noninteracting two–level systems (TLS)'s.

(c) Finally, we add the Coulomb–interaction between the electrons–holes which includes exciton and screening effects. This will lead us to the SBE's in their simplest form, including excitons or the transition to an electron hole plasma

2 Dynamics of a Two–Level–System[2]

Near resonance of an atomic transition, $\omega \approx \omega_0 = (\epsilon_2 - \epsilon_1)/\hbar$, we may only retain the pair of nearly resonant stationary states $|1\rangle$ and $|2\rangle$ with energies ϵ_1 and ϵ_2, $(\epsilon_2 > \epsilon_1)$, between which the transition occurs, see Fig. 1a. In this two–level approximation the wave function

$$|\,\psi(t)\rangle = c_1(t)|1\rangle + c_2(t)|2\rangle \tag{1}$$

is described by coefficients c_1, c_2 which may be arranged as a column vector $\boldsymbol{c}$. The time–dependence is governed by the *Schrödinger equation*

$$i\hbar\frac{\partial}{\partial t}\begin{pmatrix} c_1 \\ c_2 \end{pmatrix} = \widehat{H}\begin{pmatrix} c_1 \\ c_2 \end{pmatrix}. \tag{2}$$

In addition, we assume that the optical transition between $|1\rangle$ and $|2\rangle$ is dipole–allowed and the light is polarized parallel to the z–axis. As a result, the Hamiltonian reads

$$\widehat{H} = \widehat{H}_0 - \widehat{d}E_z(t), \qquad \widehat{H}_0 = \begin{pmatrix} \epsilon_1 & 0 \\ 0 & \epsilon_2 \end{pmatrix}, \qquad \widehat{d} = \begin{pmatrix} 0 & d^* \\ d & 0 \end{pmatrix}. \tag{3}$$

[2]The dynamics of a TLS is very well presented in many texts, in particular Allen and Eberly's classic book on *Optical Resonance and Two Level Atoms*[87A1] or the textbooks: *The Feynman lectures*, Vol. III in connection with the Ammonia maser[64F1] and *Licht und Materie* by Haken[79H2]. Note the different enumeration of states.

$\widehat{H}_0$ and $\widehat{d}$ respectively denote the Hamiltonian of the isolated atom and the electric dipole operator with $d = \langle 2| - ez|1\rangle$.

From $c_1(t), c_2(t)$ the induced dipole moment $d(t)$ and the population inversion $I(t)$ of the TLS are determined by

$$\begin{aligned} d(t) &= \mathbf{c}^\dagger \widehat{d}^* \mathbf{c} = 2\,\mathrm{Re}\,[d^*\,\mathcal{P}(t)]\,, && (4)\\ I(t) &= |c_2(t)|^2 - |c_1(t)|^2, && (5)\\ \mathcal{P}(t) &= c_1^*(t)c_2(t), && (6) \end{aligned}$$

where $\mathcal{P}(t)$ is the (dimensionless) complex dipole moment.[3] ϵ_1, ϵ_2 and d are considered as parameters of this model. There are, at least, three ways to tackle the problem which will be discussed in the next sections.

2.1 Wave–Function Description

We start with a pure state described by (1) and factor–off the time dependence of the state vector without external field (interaction picture),

$$c_j(t) = a_j(t)e^{-i\epsilon_j t/\hbar}, \quad j = 1, 2, \tag{7}$$

where $a_j(t)$ obey the differential equations

$$\dot{a}_1(t) = i\frac{d^*}{\hbar}\,E_z(t)\,e^{-i\omega_0 t}a_2(t), \quad \dot{a}_2(t) = i\frac{d}{\hbar}\,E_z(t)\,e^{+i\omega_0 t}a_1(t). \tag{8}$$

Eqs. (8) are linear and first order, nevertheless no analytical solution is achievable. However, for a monochromatic field with frequency ω near resonance, $\omega \approx \omega_0$, the product of $E_z(t) = E_0\cos(\omega t)$ and $e^{\pm i\omega_0 t}$ respectively contain a term which is almost constant and another one which oscillates rapidly. The first term drives the system coherently whereas the fast oscillating term almost averages to zero which will be neglected in the following. For reasons which will become obvious later, this approximation is called *rotating wave approximation* (RWA). Within the RWA, Eqs.(8) become

$$\dot{a}_1(t) = i\frac{\omega_R^*}{2}\,e^{+i\delta t}a_2(t), \quad \dot{a}_2(t) = i\frac{\omega_R}{2}\,e^{-i\delta t}a_1(t), \tag{9}$$

which (besides ω and ω_0) contain two characteristic frequencies

- $\omega_R = d\,E_0/\hbar$, the *Rabi-frequency* (real, for simplicity) and
- $\delta = \omega - \omega_0$, which is called the *detuning–frequency*.

[3] Haug and Koch[94H1] use a reverse notation concerning $\mathbf{P}$ and $\mathcal{P}$.

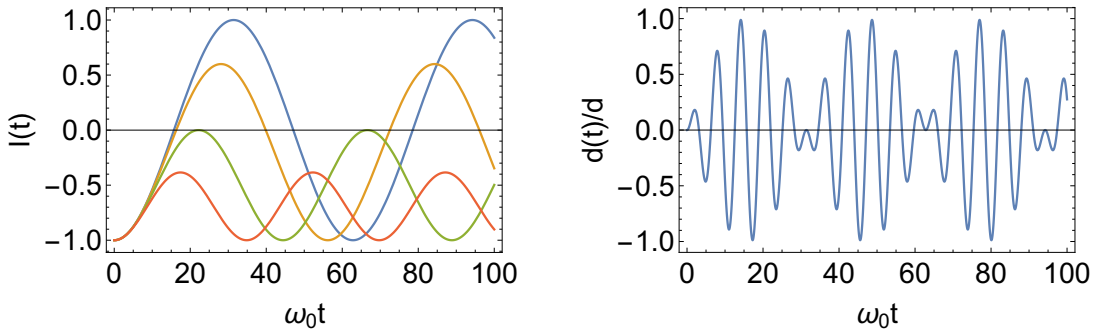

Figure 2: Rabi–oscillations of the inversion (left, $\delta = (0, 0.05, 0.1, 0.15)\omega_0$, $\omega_R = 0.1\omega_0$) and induced dipole moment (right, $\delta = 0$, $\omega_R = 0.1\omega_0$).

By insertion, Eqs. (9) lead to an equation of motion of a harmonic oscillator with "imaginary damping"

$$\ddot{a}_1(t) - i\delta\dot{a}_1(t) + (\frac{\omega_R}{2})^2 a_1(t) = 0 \tag{10}$$

which can be solved by the standard exponential Ansatz. For example, at resonance, $\delta = 0$, and initial conditions $a_1(0) = 1$, $a_2(0) = 0$, we have

$$a_1(t) = \cos(\frac{\omega_R}{2}t), \quad a_2(t) = i\sin(\frac{\omega_R}{2}t). \tag{11}$$

Hence, the probability to find the TLS in the excited state, $|c_2(t)|^2 = |a_2(t)|^2$, oscillates with the Rabi–frequency ω_R; the same holds for the population inversion, see Fig. 2. At time $t_1 = \pi/\omega_R$ the atom is in the excited state and at time $2\pi/\omega_R$ it is back again in the ground state. This is called *Rabi–flopping*. For detuned fields, the solution of (10) displays incomplete Rabi–flopping where the period becomes shorter and the amplitude is smaller than "on resonance".

A numerical example may be found, e.g., in Boyd[92B1]. For atomic sodium the parameters for the $3s-3p$ transition are: $d = 2.5a_B e$, $\lambda_0 = 589nm$. (a_B is the Bohr–radius). For an intensity of 127 Watt cm^{-2} (which can be easily realized by focussing a low power laser beam) the Rabi–frequency $\omega_R/2\pi \approx 1$GHz becomes larger than the natural line width and oscillations will show up. For further examples see, e.g., Di Bartolo's article[05D1].

2.2 Polarisation and Inversion as State–Variables

Instead of c_1, c_2 one can likewise use the inversion $I(t)$ and the complex polarisation $\mathcal{P}(t)$ themselves as state variables which – remarkably – obey a closed set of first order differential equations (without RWA!). Using Eqs. (5,6) together with Eqs.

(8) we obtain

$$\left[\frac{d}{dt}+i\omega_0\right]\mathcal{P}(t) = -i\omega_R(t)\,I(t)+\dot{\mathcal{P}}_{rel}, \quad \omega_R(t)=\frac{d}{\hbar}E_z(t), \tag{12}$$

$$\frac{dI(t)}{dt} = -4\,\mathrm{Im}\,\left[\omega_R(t)\mathcal{P}^*(t)\right]+\dot{I}_{rel}. \tag{13}$$

$\omega_R(t)$ is the instantaneous Rabi–frequency. (In the following d as well as $\omega_R(t)$ will be assumed to be real).

The advantage of this description with respect to Eqs.(8) is the possibility to include damping (i.e. incoherent interactions with a "bath") in a phenomenological way just by adding relaxation terms[4].

$$\dot{\mathcal{P}}_{rel}=-\frac{\mathcal{P}}{T_2}, \quad \dot{I}_{rel}=-\frac{I(t)-I_{eq}}{T_1}. \tag{14}$$

T_1 and T_2 determine the population (or energy) and phase relaxation of the TLS and they are also called "longitudinal" and "transverse" relaxation times. (The notation will become obvious at the end of the next section). As I is the square of an amplitude we may expect $T_2=2T_1$. However, there are always phase disturbing processes which do not contribute to energy relaxation so that in general $T_2\le 2T_1$. In semiconductors, one finds frequently that $T_2\ll 2T_1$. I_{eq} is the equilibrium value of the inversion in the absence of the driving field, e.g., at zero temperature $I_{eq}=-1$. For atoms (12,13) can be considered as optical Bloch equations.

Without damping, there is a conserved quantity,

$$4\,|\mathcal{P}(t)|^2+I^2(t)=\mathrm{const} \tag{15}$$

which may be used to eliminate the inversion from (12). Its origin becomes obvious from a remarkable analogy between a TLS and a spin–1/2 system in a magnetic field as discussed in the following subsection.

2.3 Pseudo–Spin Formulation

The Hamiltonian of a single spin–1/2 in a magnetic field $\mathbf{B}$ reads

$$\widehat{H}=-g\frac{\mu_B}{\hbar}\,\widehat{\mathbf{S}}\mathbf{B}=-\mu_B\mathbf{B}\widehat{\boldsymbol{\sigma}}, \tag{16}$$

where $\widehat{\mathbf{S}}=\frac{\hbar}{2}\widehat{\boldsymbol{\sigma}}$ is the spin-vector operator in terms of Pauli–matrices $\widehat{\sigma}_x$, $\widehat{\sigma}_y$, $\widehat{\sigma}_z$, $g=2$ is the g–factor of the electron, and μ_B is the Bohr–magneton, respectively.

When comparing (3) with (16) we conclude that any TLS is dynamically equivalent to a spin–1/2 system (zero energy such that $\epsilon_2=-\epsilon_1$). The level-splitting between the ground state and the excited state of the atom corresponds to a constant

[4] A microscopic treatment of relaxation processes requires a density matrix approach or equivalent formulations. which is not possible to do in Eqs. (8). $I(t)$ contains the diagonal elements of the density operator, $\rho_{jj}(=|c_j|^2)$, whereas $\mathcal{P}(t)$ probes the off–diagonal element $\rho_{12}(=c_1^*\,c_2)$.

magnetic field in z-direction, whereas the light field is equivalent to an oscillatory magnetic field in x–direction. The expectation value of the (pseudo–) spin operator is closely related to the complex dipole moment and the inversion:

$$S_1 = <\widehat{\sigma}_x> = c_1^* c_2 + c_1 c_2^* \quad = 2\,\mathrm{R}e\,\mathcal{P}(t), \tag{17}$$

$$S_2 = <\widehat{\sigma}_y> = -ic_1^* c_2 + ic_1 c_2^* = 2\,\mathrm{I}m\,\mathcal{P}(t), \tag{18}$$

$$S_3 = <\widehat{\sigma}_z> = \mid c_1 \mid^2 - \mid c_2 \mid^2 \; = -I(t). \tag{19}$$

The vector $\mathbf{S} = (S_1, S_2, S_3)$ obeys the (optical) *Bloch-equation*

$$\frac{d\mathbf{S}(t)}{dt} = \mathbf{\Omega} \times \mathbf{S}(t) + \dot{\mathbf{S}}_{rel}, \qquad \mathbf{\Omega} = (-2\omega_R(t), 0, -\omega_0) \tag{20}$$

which describe a rotation of $\mathbf{S}$ around vector $\mathbf{\Omega}$ at each instant of time. These equations are identical with the classical equations of motion of a spherical top in an external field (yet with fixed magnitude of the angular momentum), see Fig. 3. The relaxation term $\dot{\mathbf{\Omega}}_{sc}$ is of similar structure as in (14).

In RWA the rotation vector $\mathbf{\Omega} = (-2\omega_R \cos\omega t, 0, -\omega_0)$ is replaced by

$$\mathbf{\Omega}_{RWA} = (-\omega_R \cos\omega t, \omega_R \sin\omega t, -\omega_0) \tag{21}$$

so that the notation eventually becomes obvious: The linear polarized electromagnetic wave is decomposed in two counter–rotating circular ("pseudo–magnetic") waves and only the resonant component is retained which rotates with the same chirality as the spin vector.

In the absence of relaxation, the length of the Bloch vector is conserved, $|\mathbf{S}| = 1$ (which is equivalent to (15)) and its motion can be nicely visualized, see Fig. 3. We consider two limiting cases.

- For $\mathbf{E}(t) = 0$, $\mathbf{S}$ rotates on a cone around the z-axis which is called *L*armor-precession

$$\mathbf{S}_L(t) = \left(s_0 \sin\omega_0 t, s_0 \cos\omega_0 t, \sqrt{1 - s_0^2} \right), \quad 0 \le |s_0| \le 1. \tag{22}$$

- If the system is excited at resonance from initial state $\mathbf{S}(0) = (0, 0, 1)$ the angle of the Larmor–cone increases with time and the Bloch–vector performs a spiral motion on the unit sphere from the north– to the south pole and vice versa ("Rabi–flopping"). In RWA, we have

$$\mathbf{S}_R(t) = (\sin\omega_R t \sin\omega_0 t, \sin\omega_R t \cos\omega_0 t, \cos\omega_R t)\,. \tag{23}$$

For Rabi–frequencies comparable or even larger than the atomic transition frequency, the regime of extreme nonlinear optics is reached. Obviously, the two–level approximation is no longer well justified in this regime but, nevertheless, it seems to describe the physics fairly well. For an overview on the amazing complexity and beauty of the nonlinear optical response, see the paper by Tritschler et al.[03T1] and Ref.[24K1] (Vol. 2) for the illustration of the Bloch–dynamics.

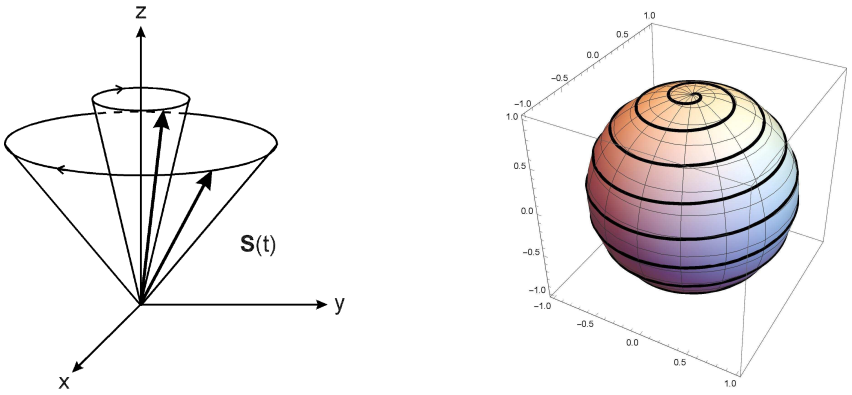

Figure 3: Larmor–precession of the Bloch–vector in a constant magnetic field $\mathbf{B} \parallel z$ (left) and Rabiflopping due to an additional superimposed *ac*– field along the 1–direction (right). Without relaxation.

2.4 Linear Response of a TLS

We are looking for a solution of Eqs. (12,13) in linear approximation with respect to the light field and zero temperature. In this case $I(t) = -1$ in (12) so that the problem to solve reduces to

$$\left[\frac{d}{dt} + (i\omega_0 + \gamma)\right] \mathcal{P}(t) = -i\frac{d}{\hbar} E_z(t), \tag{24}$$

where $\gamma = 1/T_2$. For $\mathcal{P}(-\infty) = 0$ the solution reads

$$\mathcal{P}(t) = -i\frac{d}{\hbar} \int_{-\infty}^{t} e^{-(i\omega_0+\gamma)(t-t')}\, E_z(t')\, dt'. \tag{25}$$

In particular for a monochromatic field the dipole moment (4) becomes

$$d(t) = \mathrm{Re}\, \alpha(\omega) E_0\, e^{-i\omega t}, \tag{26}$$

$$\alpha(\omega) = \frac{|d|^2}{\hbar} \left[\frac{1}{\omega_0 - (\omega + i\gamma)} + \frac{1}{\omega_0 + (\omega + i\gamma)}\right]. \tag{27}$$

$\alpha(\omega)$ is the *p*olarizability of the TLS. Remarkably, this result is almost identical with the polarizability of a classical harmonic oscillator (e.g., a particle with mass m, charge e bound to a spring with $D = m\,\omega_0^2$.)

$$\alpha_{cl}(\omega) = \frac{\frac{e^2}{m}}{\omega_0^2 - \omega^2 - 2i\gamma\omega}. \tag{28}$$

In contrast to (27), the resonance frequency of a classical oscillator shifts with increasing damping to lower values $\sqrt{\omega_0^2 - \gamma_2^2}$.

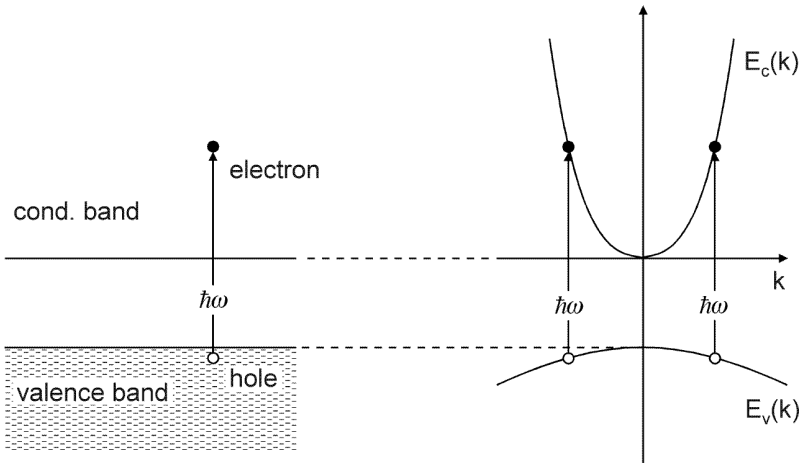

Figure 4: Two noninteracting bands viewed as a collection of TLS's with different transition energies.

3 Optical Bloch Equations

As sketched in Fig. 4 the generalization of the atomic optical Bloch–equations (12,13) to the case of a two–band semiconductor is straightforward. Neglecting the momentum of the absorbed photon, the optical transitions are vertical in $\mathbf{k}$–space. Under homogeneous conditions and neglect of scattering processes (between different $\mathbf{k}$–states in the same band) a two–band semiconductor is just an assembly of uncoupled TLS's and resembles the case of a inhomogeneously broadened line problem in atomic physics. The equations of motion are:

$$\begin{aligned} i\hbar\frac{\partial\mathcal{P}(\mathbf{k},t)}{\partial t} &= \Big[E_c(\mathbf{k})-E_v(\mathbf{k})\Big]\mathcal{P}(\mathbf{k},t) \\ &\quad +\mathbf{d}_{cv}(\mathbf{k})\mathbf{E}(t)\Big[n_c(\mathbf{k},t)-n_v(\mathbf{k},t)\Big]+i\hbar\dot{\mathcal{P}}_{rel}, \qquad (29)\\ \frac{\partial n_c(\mathbf{k},t)}{\partial t} &= -2\,\mathrm{I}m\,\Big[\mathbf{d}_{cv}(\mathbf{k})\mathbf{E}(t)\mathcal{P}^*(\mathbf{k},t)\Big]+\dot{n}_c^{rel}, \qquad (30)\\ \frac{\partial n_v(\mathbf{k},t)}{\partial t} &= +2\,\mathrm{I}m\,\Big[\mathbf{d}_{cv}(\mathbf{k})\mathbf{E}(t)\mathcal{P}^*(\mathbf{k},t)\Big]+\dot{n}_v^{rel}. \qquad (31)\end{aligned}$$

These are the semiconductor *Optical Bloch equations*. n_c, n_v are the mean occupation numbers (per spin) of the conduction and valence band Bloch states. In addition, particle conservation requires $n_c + n_v = 1$. In a phenomenological description relaxation may be included analogous to Eqs. (14). For a qualitative treatment and allowed (dipole) transitions, the $\mathbf{k}$-dependence of the interband dipole matrix element $\mathbf{d}_{cv}(\mathbf{k}) \propto \langle c,\mathbf{k}|\widehat{\mathbf{p}}|v,\mathbf{k}\rangle$ may be often neglected near the band edge. The $\mathbf{k}$–dependence is only relevant for forbidden transitions or if the variation of the polarization over the whole Brillouin–zone is needed. Note, these equations are uncoupled with respect to the wave number $\mathbf{k}$.

From $\mathcal{P}(\mathbf{k},t)$ the electronic polarization of the semiconductor can be obtained from

$$\mathbf{P}(t) = \frac{2}{V}\,\mathrm{Re}\sum_{\mathbf{k},s}\mathbf{d}^*_{cv}(\mathbf{k})\,\mathcal{P}(\mathbf{k},t), \tag{32}$$

where V denotes volume of the sample which eventually drops out when performing the sum over wave numbers in terms of an integral

$$\frac{1}{V}\sum_{\mathbf{k},s}\ldots = 2\frac{1}{(2\pi)^d}\int\ldots d^d\mathbf{k}, \tag{33}$$

where $d = 1, 2, 3$ specifies the space–dimension and the factor 2 arises from spin summation. For examples and applications see Haug–Koch[94H1] and Kalt and Klingshirn[24K1].

3.0.1 Optical Susceptibility: Interband Transitions

Next, we discuss the linear response result for the optical susceptibility of an undoped semiconductor at low temperatures and neglecting crystal anisotropy. Here n_c, n_v can be replaced by the (equilibrium) Fermi functions $f_c(k) \approx 0$, $f_v(k) \approx 1$ for the electrons in the conduction and valence bands. As $\mathbf{k}$ is merely a parameter in this approximation, the required solution of (29) can be found by the Ansatz

$$\mathcal{P}(\mathbf{k},t) = Q(\mathbf{k},t)\exp\Big[-\frac{i}{\hbar}\left(E_c(\mathbf{k}) - E_v(\mathbf{k})\right)t\Big] \tag{34}$$

with a simple integration for $Q(\mathbf{k},t)$. Eventually, we read–off the electrical susceptibility $\chi(\omega)$ from the Fourier components of $\mathbf{P}(t)$ and $\mathbf{E}(t)$ (see Problem 3).

$$\mathbf{P}(\omega) = \epsilon_0\chi(\omega)\,\mathbf{E}(\omega), \tag{35}$$

$$\chi(\omega) = \frac{1}{V\epsilon_0}\sum_{k,s}|d_{cv}(\mathbf{k})|^2\left\{\frac{f_v(\mathbf{k}) - f_c(\mathbf{k})}{E_c(\mathbf{k}) - E_v(\mathbf{k}) - \hbar(\omega + i\eta)} + \right.$$
$$\left. + \frac{f_v(\mathbf{k}) - f_c(\mathbf{k})}{E_c(\mathbf{k}) - E_v(\mathbf{k}) + \hbar(\omega + i\eta)}\right\}, \quad \eta \to +0. \tag{36}$$

For parabolic bands and $\mathbf{k}$–independent dipole matrix elements d_{cv} (along the field direction) the absorptive part of the susceptibility is proportional to the joint density of states of the valence and conduction bands. In $d = 1, 2, 3$ dimensions, the (joint) density of states and, hence, the absorption rises as $\mathrm{I}m\ \chi(\omega) \propto [\hbar\omega - E_g]^{(d-2)/2}$.

4 Semiconductor Bloch Equations

We are close to the summit of our tour towards the SBE's. Two features have not yet been taken into account:

- There is a change in Coulomb and exchange energy of the interacting many electron (ground) state when exciting an electron to the conduction band and leaving a hole behind. The main part of this interaction turns out to be an attractive Coulomb potential which adds to the external electrical field.
- With increasing band filling there is a renormalization of the electron/hole band energy by the electron/hole Coulomb interaction.

$$
\begin{aligned}
i\hbar\frac{\partial \mathcal{P}(\mathbf{k},t)}{\partial t} &= \Big[E_g + E_e(\mathbf{k}) + E_h(\mathbf{k})\Big]\mathcal{P}(\mathbf{k},t) \\
&\quad + \Big[n_e(\mathbf{k},t) + n_h(\mathbf{k},t) - 1\Big]\hbar\Omega_R(\mathbf{k},t) + i\hbar\dot{\mathcal{P}}_{rel}, \qquad (37)\\
\frac{\partial n_c(\mathbf{k},t)}{\partial t} &= -2\,\mathrm{I}m\left\{\Omega_R\mathcal{P}^*(\mathbf{k},t)\right\} + \dot{n}_c^{rel}, \qquad (38)\\
\frac{\partial n_h(\mathbf{k},t)}{\partial t} &= -2\,\mathrm{I}m\left\{\Omega_R\mathcal{P}^*(\mathbf{k},t)\right\} + \dot{n}_h^{rel}. \qquad (39)
\end{aligned}
$$

For convenience, the change in population of the valence band is formulated within the hole picture (as indicated by the index h)

$$n_v(\mathbf{k},t) = 1 - n_h(\mathbf{k},t), \qquad E_v(\mathbf{k},t) = -E_g - E_h(\mathbf{k},t). \qquad (40)$$

The factor $n_e(\mathbf{k},t) + n_h(\mathbf{k},t) - 1$ is again the population inversion at $\mathbf{k}$. Its influence on the optical absorption is often denoted as phase space filling or Pauli–blocking. The term $-2\,\mathrm{I}m\,\{\Omega_R\mathcal{P}^*(\mathbf{k},t)\}$ in Eqs. (38, 39) describes the generation of electron hole pairs by the absorption of light.

$E_e(\mathbf{k},t)$, $E_h(\mathbf{k},t)$ are the electron/hole (Hartee–Fock) energies including the interaction with other electrons/holes. For parabolic bands these are:

$$E_j(\mathbf{k},t) = \frac{\hbar^2\mathbf{k}^2}{2m_j} - \frac{1}{V}\sum_{q\ (\neq\mathbf{k})} V(\mathbf{k}-\mathbf{q})\ n_j(\mathbf{q},t), \quad j = e,h. \qquad (41)$$

Note, $m_h > 0$.

$\Omega_R(\mathbf{k},t)$ denotes the generalized Rabi–frequency (–function)

$$\hbar\Omega_R(\mathbf{k},t) = \mathbf{d}_{cv}(\mathbf{k})\mathbf{E}(t) + \frac{1}{V}\sum_{q\ (\neq\mathbf{k})} V(\mathbf{k}-\mathbf{q})\ \mathcal{P}(\mathbf{q},t), \qquad (42)$$

where $V(\mathbf{q})$ is the Fourier–transform of the (repulsive) Coulomb–potential screened by a "background" dielectric constant ϵ_b

$$V(\mathbf{q}) = \frac{e^2}{\epsilon_0\epsilon_b\, q^2}, \qquad V(\mathbf{r}) = \frac{e^2}{4\pi\epsilon_0\epsilon_b\, r}. \qquad (43)$$

Going beyond the time–dependent Hartree–Fock approximation is not easy and will need higher–order correlation functions. Physically, this leads to a further renormalization of interactions and energies which are described by four, six,... particle (e.g. biexciton,...) amplitudes, and a microscopic formulation of the relaxation terms (dephasing of the polarization, collisions of electrons and holes)[94H1, 96H1, 88Z1]. An important mechanism in this respect is the dynamical screening of the (e–e,h–h,e–h) Coulomb interactions by the excited carriers in terms of a (Lindhard–) dielectric function $\epsilon_\ell(\mathbf{q},\omega)$. Such contributions are of increasing importance for high excitation and ultrashort pulses. Moreover, in addition to the purely electronic interactions there are other scattering mechanisms, such as carrier–phonon scattering or scattering of the carriers by impurities and interface roughness in spatially confined systems. For very short times memory effects of the scattering processes come into play so that the scattering integrals in the Boltzmann equation for n_e, n_h become non–Markovian.

Further refinements of the theory may also include some details of the realistic semiconductor band–structure (e.g. more than two bands, heavy hole–light hole splitting, band–warping, ...) or spatial dispersion. At this level one is generally left with an approximate (huge) numerical effort and the problem is considered to be 'understood" or even "solved" if the results agree well with the experimental results.

4.1 Optical Susceptibility: Excitons

To demonstrate the simplicity as well as the potential of the SBE (e.g. as compared with Elliott's evaluation of the Kubo formula[57E1]) we discuss the linear optical susceptibility of the interacting electron-hole system including exciton states. At low excitation and zero temperature we have $n_v = n_h \approx 0$ so that Eqs.(37-39) reduce to:

$$i\hbar\frac{\partial\mathcal{P}(\mathbf{k},t)}{\partial t} = \Big[E_g + \frac{\hbar^2\mathbf{k}^2}{2\mu_r}\Big]\mathcal{P}(\mathbf{k},t) - \frac{1}{V}\sum_{q\,(\neq\mathbf{k})} V(\mathbf{k}-\mathbf{q})\,\mathcal{P}(\mathbf{q},t) - \mathbf{d}_{cv}\mathbf{E}(t). \quad (44)$$

μ_r denotes the reduced electron-hole mass. In distinction to the *O*ptical Bloch Equations, Eqs.(29-31), $\mathbf{k}$ is no longer just a parameter; different $\mathbf{k}$'s are coupled by $V(\mathbf{k}-\mathbf{q})$. However, this interaction term is of convolution type and, by Fourier–transformation, it reveals as the (inhomogeneous) Schrödinger–equation of the hydrogen–atom

$$i\hbar\frac{\partial\mathcal{P}(\mathbf{r},t)}{\partial t} = \Big[E_g - \frac{\hbar^2}{2\mu_r}\Delta\Big]\mathcal{P}(\mathbf{r},t) - V(\mathbf{r})\mathcal{P}(\mathbf{r},t) - \mathbf{d}_{cv}\,\mathbf{E}(t)\,\delta(\mathbf{r}). \quad (45)$$

Eq. (45) is also known as the Wannier–Equation, $\mathcal{P}(\mathbf{r},t)$ plays the part of the exciton (envelope) wave–function. The $\mathbf{k}$–dependence of the interband matrix element $\mathbf{d}_{cv}(\mathbf{k})$ has been neglected.

For $\mathbf{E} = 0$ the stationary states are well known from standard texts on Quantum Mechanics

$$\mathcal{P}_\alpha(\mathbf{r},t) = e^{-i\frac{E_\alpha}{\hbar}t}\,\Psi_\alpha(\mathbf{r}), \quad E_\alpha = -\frac{Ry^*}{n^2}, \quad Ry^* = Ry\,\frac{\mu_r/m_0}{\epsilon_b^2}. \tag{46}$$

$Ry = 13.56\ldots$eV is the hydrogenic Rydberg energy.[5] Quantum numbers $\alpha = (n,l,m)$ have their usual meaning and, formally, n labels the discrete as well as the continuum states. In a semiconductor, these (bound) hydrogenic states are called *excitons* which have been extensively discussed in the literature, see in particular Vol. 2 of Kalt and Klingshirn's book[24K1] and the references cited therein.

For $\mathbf{E}(t) \neq 0$ (parallel to the z–direction) we seek the solution of $\mathcal{P}(\mathbf{r},t)$ in terms of the complete set of the stationary states as given by (46),

$$\mathcal{P}(\mathbf{r},t) = \sum_\alpha Q_\alpha(t)\,\mathcal{P}_\alpha(\mathbf{r},t), \tag{47}$$

where $Q_\alpha(t)$ can be found by a simple integration

$$Q_\alpha(t) = i\frac{d_{cv}}{\hbar}\,\Psi^*_\alpha(\mathbf{r}=0)\,\int_{-\infty}^{t} E_z(t')\,e^{i\frac{E_\alpha}{\hbar}t'}e^{\eta t'}\,dt', \quad \eta \to 0^+. \tag{48}$$

$\exp(\eta t)$ has been added to switch–on the light at $t = -\infty$ adiabatically. Obviously, the (spatially constant) light–field creates only those exciton states which have a nonvanishing wave function at the origin; these are the s–states.[6]

Inserting (47) in (33) and using the completeness relation of the stationary states (46), we finally obtain the electrical susceptibility (isotropic approximation, d_{cv} along $\mathbf{E}$)

$$\begin{aligned}\chi(\omega) &= 2\frac{|d_{cv}|^2}{\epsilon_0}\,\sum_\alpha |\Psi_\alpha(\mathbf{r}=0)|^2\left\{\frac{1}{E_g + E_\alpha - \hbar(\omega+i\eta)} + \right.\\ &\left. + \frac{1}{E_g + E_\alpha + \hbar(\omega+i\eta)}\right\}.\end{aligned} \tag{49}$$

In a bulk semiconductor the absorptive part consists of a series of delta–functions at the bound exciton s–states with rapidly decreasing oscillator strength $\propto n^{-3}$ and a continuum part[94H1]

$$Im\;\chi(\omega) \propto \sum_{n=1}^{\infty}\frac{4\pi}{n^3}\delta(\Delta + \frac{1}{n^2}) + \theta(\Delta)\,\frac{\pi\exp\left(\frac{\pi}{\sqrt{\Delta}}\right)}{\sinh(\frac{\pi}{\sqrt{\Delta}})}. \tag{50}$$

[5] If the excitonic Rydberg Ry^* is smaller than the LO–phonon energy, ϵ_b is given by the static dielectric constant ϵ_s, otherwise by ϵ_∞.

[6] This result originates from our approximation $\mathbf{d}_{cv}(\mathbf{k})$=const. If the dipole element vanishes linearly with $\mathbf{k}$ at the band edge the coupling is solely to p–states. A prominent example is Cu_2O, see Sect. 15.3.1 of Ref.[24K1] (Vol. 2) and Problem 4.

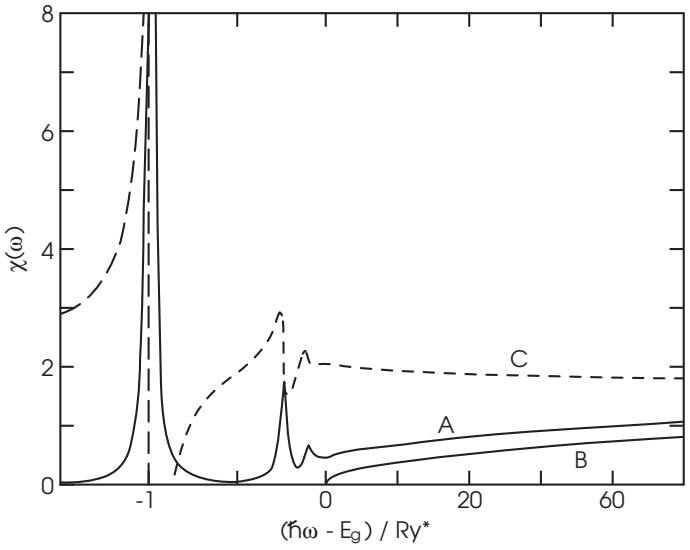

Figure 5: Electrical susceptibility of a direct semiconductor near the gap energy: (A) I$m\,\chi$, (C) R$e\,\chi$ of the interacting electron hole system, (50), (B) I$m\,\chi$ of the noninteracting system, (36). Note the different frequency scale above and below the gap. An appropriate broadening was included phenomenologically. According to Stahl and Balslev [87S1].

$\Delta = (\hbar\omega - E_g)/Ry^*$ denotes the normalized photon energy. Close to the ionization continuum, $\Delta \to 0$, the absorption raises step–like in striking distinction to the square–root law for noninteracting bands, cf. (36). Thus, the attractive Coulomb interaction not only creates bound states below the gap but leads to a pronounced enhancement of the absorption above the gap (so called Sommerfeld–enhancement). Eq. (50) was first derived by Elliott [57E1] but on a much more elaborate way. (The corresponding real part can be calculated from Kramers–Kronig relations.)

The optical absorption spectrum bulk $GaAs$ is displayed in Fig. 5 which gives a lively impression about the importance of the Coulomb interaction and exciton states near the band gap. In the very best samples exciton lines up to $n = 3$ can be resolved in this material. A rich collection of excitonic data on various semiconductors and systems can be found in Kalt and Klingshirn's book[24K1].

4.2 Photon Echo

The analogy of a TLS with the Spin–1/2 problem offers an unexpected insight in an interesting phenomenon which is called *photon–echo*. Here, we examine the rather marvellous notion that not all macroscopic decay processes are irreversible.[7] Usually, in an experiment many TLS are involved and because of different local environments

[7]This technique was developped by Hahn [50H1] for nuclear spin systems and it plays an important role to measure the T_2–time. For a thorough discussion we refer to Chap. 9 of Allen and Eberly [87A1] and to Sect. 11.4 of Kalt and Klingshirn's book[24K1] for experimental results.

these have individually slightly different transition frequencies (=inhomogeneous line broadening, spectral width is parameterized by $1/T_2^*$). Hence, the macroscopic (magnetization or polarization) signal contains many contributions with slightly different frequencies which add up almost to zero in a rather short time ($\approx T_2^*$), yet the individual systems are still oscillating with a fixed phase relation with respect to the exciting pulse and the energy stored in the moments being out of phase can be recovered in a coherent fashion. Instead of waiting for the extremely unlikely Poincaré–recurrence of the initial state, a second pulse after time T is used which – loosely speaking – causes a "time reversal operation" which is followed by an echo of the initial puls after total time $2T$.

To uncover the echo phenomenon it is convenient to describe the dynamics of the Bloch–vector in a frame rotating with the frequency of the light (not the atomic transition frequency!) around the 3–axis:

$$\begin{aligned} R_1(t) &= S_1(t)\cos\omega t - S_2(t)\sin\omega t, && (51)\\ R_2(t) &= S_1(t)\sin\omega t + S_2(t)\cos\omega t, && (52)\\ R_3(t) &= S_3(t). && (53) \end{aligned}$$

(In complex notation the $1,2$ components can be summarized by $R = R_1 + iR_2$, $S = S_1 + iS_2$, with $R = Se^{i\omega t}$.) In this frame the equations of motion read

$$\begin{aligned} \dot{R}_1(t) &= -\delta R_2(t) - \frac{R_1(t)}{T_2}, && (54)\\ \dot{R}_2(t) &= +\delta R_1(t) + \omega_R R_3(t) - \frac{R_2(t)}{T_2}, && (55)\\ \dot{R}_3(t) &= -\omega_R R_2(t) - \frac{R_3(t) - R_3^{eq}}{T_1}. && (56) \end{aligned}$$

These linear differential equations have constant coefficients so that the solution can be found by an exponential Ansatz. In particular, for $\omega_R = 0$ the Bloch–vector performs a (damped) Larmor–precession around the 3–axis:

$$\begin{aligned} R_1(t) &= [R_1(0)\cos\delta t - R_2(0)\sin\delta t]\; e^{-\frac{t}{T_2}}, && (57)\\ R_2(t) &= [R_1(0)\sin\delta t + R_2(0)\cos\delta t]\; e^{-\frac{t}{T_2}}, && (58)\\ R_3(t) &= R_3^{eq} + [R_3(0) - R_3^{eq}]\; e^{-\frac{t}{T_1}}. && (59) \end{aligned}$$

At resonance, $\delta = 0$, but neglecting damping, a light pulse causes a Rabi–rotation of the Bloch–vector around the 1–axis

$$\begin{aligned} R_1(t) &= +R_1(0), && (60)\\ R_2(t) &= +R_2(0)\cos\omega_R t + R_3(0)\sin\omega_R t, && (61)\\ R_3(t) &= -R_2(0)\sin\omega_R t + R_3(0)\cos\omega_R t. && (62) \end{aligned}$$

In the discussion of a photon–echo experiment four periods have to be distinguished, see Fig. (6). To simplify matters, we shall assume that the pulse duration

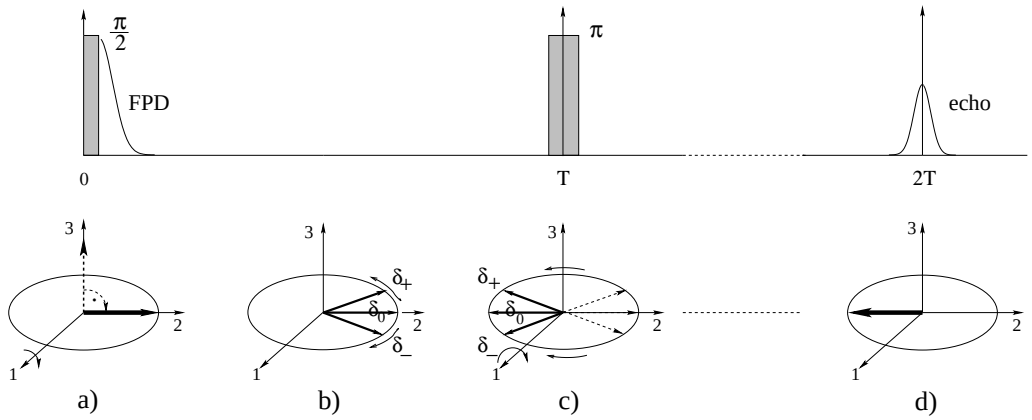

Figure 6: Principle of a photon echo experiment. Upper part: Standard pulse sequence (dashed blocks, duration exaggerated) and resulting polarization (solid lines). Lower part: Dynamics of the Bloch–vector in the rotating frame a) Alignment of the individual Bloch–vectors along the 2–direction by a $\pi/2$–rotation around the 1–axis. b) Precession of the individual Bloch–vectors in the 1–2 plane as determined by their various detunings leading to the free polarization decay (FPD). c) π–rotation around the 1–axis transforms $R_2 \to -R_2$ but leaves R_1 unchanged. d) Reproduction of the initial state at time T after the π–pulse. (For simplicity only 3 Blochvectors are displayed with detunings $\delta_+ > 0$, $\delta_0 = 0$, $\delta_- < 0$).

is short with respect to T_1, T_2, T_2^* and intense, $\omega_R T_2^* \gg 1$, so that the influence of damping and detuning can be safely neglected during the pulses.

1. All TLS start from the same initial state $\mathbf{R}^{(0)} = (0, 0, 1)$. Then the ensemble of atoms is polarized by a first light pulse (duration τ_1) which, according to Eqs. (60-62), leads to a common Bloch vector $\mathbf{R}^{(1)} = (u, v, w)$. For a socalled $\pi/2$–pulse, i.e. $\phi_1 = \omega_R \tau_1 = \pi/2$, the polarization (magnetization) is "tipped" to the 2-direction: $\mathbf{R}^{(1)} = (0, 1, 0)$. See Fig. 6a.

2. After the first light pulse the individual Bloch-vectors $\mathbf{R}^{(2)}$ precess according to Eqs. (57-59). Because of their slightly different frequencies the individual dipole moments get out of phase (relative to each other) and add to zero in a time T_2^* which is much shorter than T_2. This dephasing phenomenon is called $f$ree polarization decay (FPD). See Fig. 6b. (Since we are in a rotating frame only the phase deviations relative to $\exp(-i\omega t)$ appear in this figure.)

3. After time T a second light pulse is applied (duration τ_2, phase $\phi_2 = \omega_R \tau_2$) which according to Eqs. (60 - 61) "tips" the polarization to $\mathbf{R}^{(3)}$.

4. After the second pulse the Bloch–vectors $\mathbf{R}^{(4)}$ again rotate freely around the

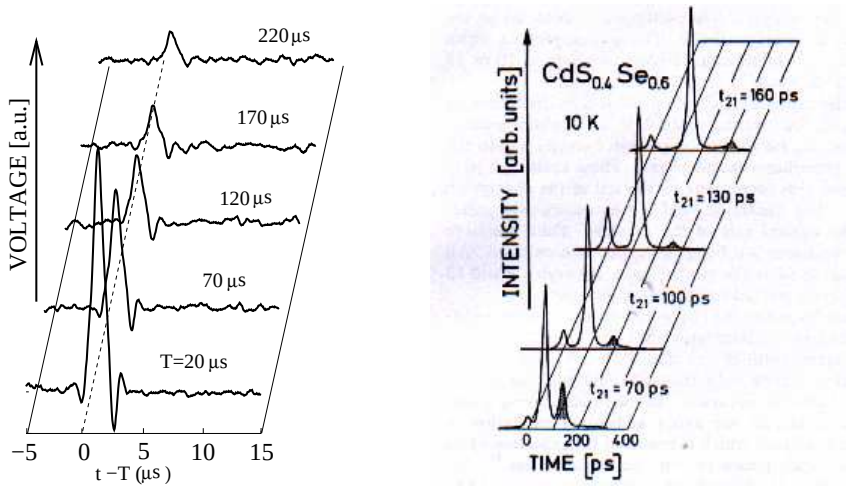

Figure 7: Experimental spin–echo for protons in water ($\omega/2\pi$ = 95MHz, duration of π–pulse: 1.4μs, $T_2 \approx 75\mu$s, $T_2^* \approx 1\mu$s, $T_1 \approx 10$s, room temperature)[03F1] (left) and photon echo in a II-VI semiconductor compound[92S1](right).

3–axis. As a result, we obtain for the 2–component

$$R_2^{(4)}(t) = \Big\{ u\left[\cos\delta T \sin\delta t + \cos\phi_2 \sin\delta T \cos\delta t\right] \tag{63}$$

$$-v\left[\sin\delta T \sin\delta t - \cos\phi_2 \cos\delta T \cos\delta t\right] \Big\} e^{-\frac{t+T}{T_2}} \tag{64}$$

$$+\sin\phi_2 \cos\delta t \left[1 + (w-1)\, e^{-T/T_1}\right]\ e^{-T/T_2}, \tag{65}$$

where the time t counts from the end of the second pulse. For $\phi_2 = \pi$ the terms in the [..] brackets combine to $\cos\delta(T-t)$ and $\sin\delta(T-t)$ and all individual Bloch–vectors again are in phase at time $2T$ after the first pulse and add up to a macroscopic polarization. This causes the emission of a light pulse, the *p*hoton–echo.

The resurrected free polarization signal has the magic quality of something coming from nothing. However, this resurrection is only possible for times which are comparable with the T_2–time. For larger times, the intensity of the photon–echo decays as the square of $\exp(-2T/T_2)$ i.e. $\exp(-4T/T_2)$. T_2 is also called *decoherence or dephasing time*.

It is interesting that the existence of the echo is not attributed to the π–character of the second pulse as it is frequently imputed. When decomposing the products of trigonometric functions $\cos\delta T \cos\delta t$ etc., in terms of sum and differences we realize that there is a contribution to the polarization of the form:

$$R_2^{(4)} = -\frac{1-\cos\phi_2}{2}\Big\{ u\sin\left[\delta(T-t)\right] + v\cos\left[\delta(T-t)\right]\Big\} e^{-\frac{t+T}{T_2}} + \ldots \tag{66}$$

Thus, a second pulse of *a*ny duration will induce an echo. However, its intensity is largest for $\phi_2 = \pi$ (and $\phi_1 = \pi/2$). (Terms omitted in (66) indicate non–echo contributions).

Although spin and photon echo phenomena have the same theoretical roots, there are profound experimental differences.

- In semiconductors, photon–echos are generated with light pulses which correspond to phase shifts much smaller than π. $\Phi = \pi$ would lead to a complete band inversion which, in turn, would lead to a collapse of the semiconductor bandstructure. This regime is hardly accesssible and would generate additional fast dephasing processes.

- Spin–echos are generated with rf or microwave fields with wavelength much larger than the dimensions of the specimen. The situation is opposite for photon–echos in semiconductors where standard experimental techniques, e.g. four wave mixing, uses pulses travelling in different directions so that the echo signal can be spatially separated from the exciting pulses. Details are discussed in Ref. [24K1] (Vol. 2).

A popular analogy of the spin–echo phenomenon and a group of runners in a stadion is discussed in Chap. 9 of Allen and Eberly's book [87A1]. However, it should be kept in mind that a π–rotation around the 1–axis at time T causes a reconfiguration of the pulse – analogous to optical phase conjugation – rather than a time–reversal of the dynamics of the individual Bloch vectors.

Experimentally, photon–echo measurements are often used as a tool to determine the optical dephasing rate T_2. In semiconductors systems, however, the (dynamically screened) interactions of the electron hole pairs may lead to significant deviations from the atomic case and the analysis of experimental results requires a detailed numerical study of the SBE's which has been first undertaken by Lindberg et al.[92L1]. For an overview and details see Haug and Koch[94H1] and Schäfer and Wegener[02S1]. A rich collection of data about applications of this technique on various semiconductors and systems can be found in Kalt and Klingshirn's book[24K1] (Vol. 2). An easy readable review on the spin and photon–echo in semiconductors as well as an overview on related echo–phenomena has been published by Meier and Thomas[03M1].

A preliminary version of this article has been published in the proceedings of an Erice Summer School[98B1] and in previous editions of Ref. [24K1].

5 Problems

1. Solve (10) for arbitrary detuning and calculate the wave function coefficients $c_j(t)$ (or $a_j(t)$), inversion $I(t)$, and complex polarization $\mathcal{P}(t)$. Initial conditions are $c_1(0) = 1$, $c_2(0) = 0$.

2. At resonance there are "stationary" states of the coupled TLS–electrical field, Eqs. (10), with time–independent probabilities $|c_j(t)|^2$=const. Find these "dynamical Stark–states".

3. Use the Ansatz proposed by (34) to solve Eqs. (29) for a monochromatic field and derive the interband susceptibility $\chi(\omega)$ given by (36).
   Hint: In the absence of damping the light field must be switched–on adiabatically at $t = -\infty$, $\mathbf{E}(t) = E_0 \exp(\eta t) \cos(\omega t)$, $\eta \to +0$. Otherwise the response contains spurios contributions from the physically irrelevant inital state.

4. If the transitions near the band–edge are forbidden (in first order) the dipole matrix element behaves as $\mathbf{d}_{cv}(\mathbf{k}) \propto \mathbf{k}$. Show that the optical absorption is now linked to exciton p–states.
   Hints: For $r \to 0$ hydrogenic wave functions behave as $\Psi_{n,l,m}(r, \theta, \phi) \propto r^l$. Under Fouriertransformation: $grad \to i\mathbf{k}$.

5. Find the general solution of the Bloch equations for the photon–echo problem, Eqs. (54-56). Express the integration constants in terms of the Bloch–vector at $t = 0$, $\mathbf{R}(0)$.
   Hint: The solution can be obtained by an exponential Ansatz with $\mathbf{R}(t) = \boldsymbol{\rho} \exp(\lambda t)$, where $\boldsymbol{\rho}$ is a time–independent 3–component vector.

6. Photon–echo with pulses of equal duration, i.e. $\Phi = \Phi_1 = \Phi_2$. Show that the echo signal is maximal for $\Phi = 2\pi/3$ and even a bit stronger than for the $\pi/2$–π sequence.

References

[46B1] F. Bloch, Phys. Rev. **70**, 460 and 474 (1946).

[50H1] E. L. Hahn, Phys. Rev. **8**0, 580 (1950).
See also: *Nonlinear Spectroscopy of Solids, Advances and Applications*, B. Di Bartolo (ed.), Nato ASI Series B, Vol. 339, page 75, Plenum (1994).

[57E1] R. J. Elliott, Phys. Rev. **1**08, 1384 (1957).
See also: *Polarons and Excitons*, edited by C. G. Kuper and G. D. Whitfield, Oliver and Boyd (1963).

[64F1] R. P. Feynman, R. B. Leighton, M. Sands, *The Feynman Lectures on Physics*, Vol. III, Addison–Wesley (1964).

[70H1] H. Haken, in: Handbuch der Physik, *Light and Matter 1c*, Vol. XXV/2c, S. Flügge (ed.), Springer (1970).

[79H2] H. Haken, *Licht und Materie*, Vol. 2, Bibliographisches (1979).

[84S1] A. Stahl, Solid State Commun. **49**, 91 (1984).

[87A1] L. Allen, J. H. Eberly, *Optical Resonance and Two–Level Atoms*, Dover (1987).

[87S1] A. Stahl, I. Balslev, *Electrodynamics of the Semiconductor Band Edge*, Springer Tracts in Modern Physics, Vol.110, Springer (1987).

[88Z1] R. Zimmermann, *Many Particle Theory of Highly Excited Semiconductors*, Teubner (1988).

[92B1] R. W. Boyd, *Nonlinear Optics*, Academic Press (1992).

[92L1] M. Lindberg, R. Binder, S. W. Koch, Phys. Rev. A **45**, 1865 (1992).

[92S1] U. Siegner, D. Weber, E. O. Göbel, D. Bennhardt, V. Heukeroth, R. Saleh, S. D. Baranovskii, P. Thomas, H. Schwab, C. Klingshirn, J. M. Hvam, V. G. Lyssenko, Phys. Rev. **B** 46, 4564 (1992).

[94H1] H. Haug, S. W. Koch, *Quantum Theory of the Optical and Electronic Processes of Semiconductors*, 5^{th} Ed., World Scientific (2009).

[96H1] H. Haug, A–P. Jauho, *Quantum Kinetics in Transport and Optics of Semiconductors*, Springer (1996).

[96S1] J. Shah, *Ultrafast Spectroscopy of Semiconductor and Semiconductor Nanostructures*, Springer Series in Solid State Sciences, **115**, (1996).

[98B1] R. v. Baltz, in: *Ultrafast Dynamics of Quantum Systems: Physical Processes and Spectroscopic Techniques*, B. Di Bartolo ed., Nato ASI series B, Vol. 372, Plenum (1998).

[02S1] W. Schäfer, M. Wegener, *Semiconductor Optics and Transport Phenomena*, Advanced Texts in Physics, Springer (2002).

[03F1] F. Fujara, Ch. Köhler, private communication, Institut für Festkörperphysik, Technische Universität Darmstadt.

[03L1] V. Lyssenko, D. Meinhold, B. Rosam, K. Leo, D. Birkedal, J. Erland, M. van der Poel, J. Hvam, *Coherent Spectroscopy of Semiconductor Microcavities*, in Ref.[05D1].

[03M1] T. Meier, P. Thomas, *Echos in Festkörpern*, Physik Journal, März issue, p. 53, Wiley–VCH (2003).

[03T1] T. Tritschler, O. D. Mücke, M. Wegener, Phys. Rev. A **68**, 33404 (2003).

[05D1] B. Di Bartolo, in: *Investigating Extreme Physical Conditions with Advanced Optical Techniques*, B. Di Bartolo ed., Nato ASI series II, Springer (2005).

[24K1] H. Kalt, C.F Klingshirn, *Semiconductor Optics*, Vol. 1,2, 5^{th} Ed., Springer (2024).

... updated Sept 17, 2024 ...